A Climatology of Tropospheric Zonal-Mean Water Vapor Fields and Fluxes in Isentropic Coordinates

TAPIO SCHNEIDER, KAREN L. SMITH, PAUL A. O'GORMAN, AND CHRISTOPHER C. WALKER*

California Institute of Technology, Pasadena, California

(Manuscript received 5 January 2006, in final form 27 February 2006)

ABSTRACT

Based on reanalysis data for the years 1980–2001 from the European Centre for Medium-Range Weather Forecasts (ERA-40 data), a climatology of tropospheric zonal-mean water vapor fields and fluxes in isentropic coordinates is presented. In the extratropical free troposphere, eddy fluxes dominate the meridional flux of specific humidity along isentropes. At all levels, isentropic eddy fluxes transport water vapor from the deep Tropics through the subtropics into the extratropics. Isentropic eddy fluxes of specific humidity diverge near the surface and in the tropical and subtropical free troposphere; they converge in the extratropical free troposphere. Isentropic mean advective fluxes of specific humidity play a secondary role in the meridional water vapor transport in the free troposphere; however, they dominate the meridional flux of specific humidity near the surface, where they transport water vapor equatorward and, in the solstice seasons, across the equator. Cross-isentropic mean advective fluxes of specific humidity are especially important in the Hadley circulation, in whose ascending branches they moisten and in whose descending branches they dry the free troposphere.

Near the minima of zonal-mean relative humidity in the subtropical free troposphere, the divergence of the cross-isentropic mean advective flux of specific humidity in the descending branches of the Hadley circulation is the dominant divergence in the mean specific humidity balance; it is primarily balanced by convergence of cross-isentropic turbulent fluxes that transport water vapor from the surface upward. Although there are significant isentropic eddy fluxes of specific humidity through the region of the subtropical relative humidity minima, their divergence near the minima is generally small compared with the divergence of cross-isentropic mean advective fluxes, implying that moistening by eddy transport from the Tropics into the region of the minima approximately balances drying by eddy transport into the extratropics. That drying by cross-isentropic mean subsidence near the subtropical relative humidity minima is primarily balanced by moistening by upward turbulent fluxes of specific humidity, likely in convective clouds, suggests cloud dynamics may play a central role in controlling the relative humidity of the subtropical free troposphere.

1. Introduction

Water vapor fields and fluxes in the troposphere are affected by processes on many scales. The specific humidity in the boundary layer is directly related to evaporation from the surface. From the boundary layer, water vapor is transported upward by large-scale eddies and, particularly in the deep Tropics, by convection. Transport and evaporation of condensate moistens the vicinity of moist-convective regions (see, e.g., Sun and Lindzen 1993; Emanuel and Pierrehumbert 1995). Sufficiently far away from regions of moist convection, however, large-scale processes play an essential role in the hydrologic cycle of the free troposphere: mean circulations and large-scale eddies advect moist air originating in the boundary layer or in regions of moist convection into colder regions, where the air reaches saturation, water vapor condenses, and precipitation occurs; large-scale subsidence brings drier air from upper levels of the atmosphere into lower levels; and large-scale eddies mix drier air with moister air (see, e.g., Yang and Pierrehumbert 1994; Sherwood 1996a,b; Salathé and Hartman 1997; Pierrehumbert and Roca

* Current affiliation: Department of Earth and Planetary Science, Harvard University, Cambridge, Massachusetts.

Corresponding author address: Tapio Schneider, California Institute of Technology, Mail Code 100-23, 1200 E. California Blvd., Pasadena, CA 91125.
E-mail: tapio@caltech.edu

1998; Soden 1998; Dessler and Sherwood 2000; Pierrehumbert 2002; Pierrehumbert et al. 2006).

The relative importance of different large-scale processes, such as large-scale eddies and mean subsidence, in the hydrologic cycle of the troposphere is not completely known. For example, it has long been held that mean subsidence in the descending branches of the Hadley circulation is responsible for the relative dryness of the subtropical free troposphere. Alternatively, however, the subtropics can be dehydrated by large-scale eddy transport (Kelly et al. 1991; Yang and Pierrehumbert 1994). Consider adiabatic advection of a moist subtropical air mass through one turnover time of a large-scale eddy, embedded in a statically stable environment in which temperature decreases upward and poleward. Initially, the eddy advects the subtropical air mass poleward, approximately along an upward sloping dry entropy surface, until, in a colder region at higher latitudes and higher altitudes, the air reaches saturation, water vapor condenses, and precipitation occurs. Further poleward advection of the saturated air mass into yet colder regions will be approximately confined to a saturated entropy surface and will be associated with further condensation and precipitation. When the meridional velocity reverses, the eddy advects the air back toward the equator into warmer regions, again approximately along a dry entropy surface. During the downward sloping equatorward advection, the specific humidity of the air mass is conserved at the value at the point of last saturation, provided water vapor sources such as evaporation of condensate can be neglected. When the air mass returns to its original latitude, even if the eddy dynamics are reversible up to latent heat release, the air mass will have the specific humidity of its point of last saturation and so will generally, if precipitation occurred, be drier than the original air mass. The eddy has transported water vapor from the subtropics into higher latitudes. The time scale of mean subsidence is the radiative time scale, which is on the order of 10 days, whereas the turnover time of large-scale eddies is on the order of a few days. So one may suspect that much of the air in the region of the subtropical relative humidity minima, to the extent that the time scale of eddy incursions into that region lies between the eddy turnover time and the radiative time scale, was last saturated at higher latitudes and altitudes. Galewsky et al. (2005) show that this is indeed the case: in the zonal mean, according to reanalysis data for December–January–February 2001–02, about half of the air in the region of the subtropical relative humidity minima in the Northern Hemisphere was last saturated at points poleward of that region, primarily at points lying on the mean isentrope going through the region. There clearly are significant, approximately isentropic, eddy fluxes of water vapor from the subtropics into higher latitudes. However, Galewsky et al. also show that a substantial fraction of the air in the region of the subtropical relative humidity minima was last saturated at lower latitudes and higher altitudes, implying that there are also significant fluxes of water vapor from the Tropics into the subtropics, as well as cross-isentropic subsidence of relatively dry air. The magnitude and global structure of the implied isentropic and cross-isentropic fluxes of water vapor are unknown.

Based on European Centre for Medium-Range Weather Forecasts (ECMWF) reanalysis data for the years 1980–2001, here we present a climatology of zonal-mean water vapor fields and fluxes and their seasonal variations in isentropic coordinates. Analyzing water vapor fluxes in isentropic coordinates provides a clear separation between diabatic processes, such as mean subsidence, and approximately adiabatic processes, such as transient airmass displacements in large-scale eddies. To the extent that airmass displacements in large-scale eddies approximately follow dry entropy surfaces—that is, to the extent that it can be ignored that saturated ascent follows saturated rather than dry entropy surfaces—averages of transport statistics in isentropic coordinates yield approximations of the Lagrangian mean transport (see, e.g., Johnson 1989), thus complementing direct studies of Lagrangian transport such as that of Galewsky et al. (2005).

Section 2 discusses the theoretical framework of our analyses, the water vapor balance in isentropic coordinates. Section 3 describes the data and analysis methods. Section 4 presents mean fields and decompositions of fluxes and their divergences in isentropic coordinates. Section 5 summarizes the conclusions and discusses implications of the findings for Earth's hydrologic cycle.

2. Water vapor balance in isentropic coordinates

The basis of the analyses is the balance equation for water vapor in isentropic coordinates,

$$\partial_t(\rho_\theta q) + \nabla_\theta \cdot (\rho_\theta \mathbf{v} q) + \partial_\theta(\rho_\theta Q q) = \rho_\theta S, \qquad (1)$$

where q is the specific humidity, $\mathbf{v} = (u, v)$ the horizontal velocity with eastward component u and northward component v, $Q = D\theta/Dt$ the diabatic heating, θ potential temperature, and $\nabla_\theta \cdot$ denotes the horizontal divergence along isentropes. The isentropic density $\rho_\theta = -g^{-1}\partial_\theta p\, \mathcal{H}(\theta - \theta_s)$ is the density in isentropic coordinates; that is, $\rho_\theta\, dx\, dy\, d\theta$ is the mass of moist air enclosed in the isentropic-coordinate volume element $dx\, dy\, d\theta$. The Heaviside step function $\mathcal{H}(\cdot)$ in the isen-

tropic density represents Lorenz's (1955) convention of setting the isentropic density to zero on isentropes with potential temperature θ less than the instantaneous surface potential temperature $\theta_s = \theta_s(x, y, t)$. This convention ensures that the balance equation (1) holds on isentropes both above the surface ($\theta \geq \theta_s$) and "inside" the surface ($\theta < \theta_s$), where it reduces to the trivial statement $0 = 0$. We view the horizontal flux term on the left-hand side of the balance equation (1) as representing fluxes resolved in the reanalysis data, so that the source-sink term S on the right-hand side is the difference between the local rates of evaporation and condensation, plus contributions from parameterized subgrid-scale processes such as small-scale turbulent dispersion of water vapor. The diabatic heating Q includes radiative heating/cooling as well as parameterized subgrid-scale processes such as latent heat release in moist convection or in large-scale condensation. [See Peixoto and Oort (1992, chapter 12.2.2) for the water vapor balance equation and Johnson (1989) or Schneider et al. (2003) for the transformation of balance equations to isentropic coordinates.]

Averaging the balance equation (1) zonally and temporally (e.g., over a month or a season) along isentropes yields

$$\partial_t(\overline{\rho}_\theta\, \overline{q}^*) + \partial_y(\overline{\rho}_\theta\, \overline{vq}^*) + \partial_\theta(\overline{\rho}_\theta\, \overline{Qq}^*) = \overline{\rho}_\theta\, \overline{S}^*, \qquad (2)$$

where $\overline{(\cdot)}^* = \overline{(\rho_\theta\, \cdot)}/\,\overline{\rho}_\theta$ denotes the mass-weighted mean associated with the mean $\overline{(\cdot)}$ along isentropes. [We use the local Cartesian meridional derivative ∂_y symbolically to simplify the notation; however, in all actual calculations, we use the spherical-coordinate version of the meridional divergence along isentropes, $\partial_y(\cdot) \leftarrow (a\, \cos\phi)^{-1}\partial_\phi(\cdot\, \cos\phi)$ with latitude ϕ and Earth's radius a.] With the convention of setting the isentropic density to zero on isentropes inside the surface, the mean balance equation (2) holds throughout the flow domain in isentropic coordinates, including the surface layer of isentropes that sometimes intersect the surface (cf. Schneider 2005). In particular, vertical integrals over potential temperature of quantities weighted by the isentropic density are equal to mass-weighted integrals over height. For example, the integral $\int_{\theta_b}^{\infty} \overline{\rho}_\theta\, \overline{q}^*\, d\theta$, with a nominal lower-boundary potential temperature θ_b less than or equal to the smallest potential temperature that occurs at a given latitude, is the mean precipitable water, or the mean mass of water vapor per unit area in an atmospheric column.

The mean fluxes along isentropes $\overline{vq}^*$ and across isentropes $\overline{Qq}^*$ approximate the mean Lagrangian transport of water vapor in the meridional plane. If changes in specific humidity over the averaging period can be neglected, the divergence of this approximately Lagrangian transport balances the source-sink term $\overline{\rho}_\theta\, \overline{S}^*$. The mean balance equation (2) gives a statistical description of the ensemble of trajectories leading from source regions of water vapor to regions of condensation—a statistical description of the trajectories explored in several case studies (e.g., Sherwood 1996b; Salathé and Hartman 1997; Pierrehumbert and Roca 1998; Soden 1998; Dessler and Sherwood 2000).

If one decomposes the flux ($\overline{vq}^*$, $\overline{Qq}^*$) of water vapor into mean components ($\overline{v}^*\, \overline{q}^*$, $\overline{Q}^*\, \overline{q}^*$) and eddy components ($\overline{v'q'}^*$, $\overline{Q'q'}^*$), where primes denote fluctuations $(\cdot)' = (\cdot) - \overline{(\cdot)}^*$ about the mass-weighted isentropic mean, the mean balance equation (2) becomes

$$\partial_t(\overline{\rho}_\theta\, \overline{q}^*) + \partial_y(\overline{\rho}_\theta\, \overline{v}^*\, \overline{q}^*) + \partial_\theta(\overline{\rho}_\theta\, \overline{Q}^*\, \overline{q}^*) = \overline{\rho}_\theta\, \overline{S}^* - \partial_y(\overline{\rho}_\theta\, \overline{v'q'}^*) - \partial_\theta(\overline{\rho}_\theta\, \overline{Q'q'}^*). \qquad (3)$$

This decomposition of the mean balance equation provides the conceptual framework for our analyses of water vapor transport in the troposphere. The flux terms on the left-hand side represent the mean advection of specific humidity by the overturning mass transport circulation in isentropic coordinates. The flux terms on the right-hand side represent divergences of the eddy fluxes of specific humidity along and across isentropes.

Averaging water vapor fluxes along dry isentropes only gives an approximation of the Lagrangian water vapor fluxes. Displacements in large-scale eddies in the free troposphere are not exactly confined to dry isentropes but, if other diabatic processes on eddy turnover time scales are negligible, approximately follow saturated moist entropy surfaces in saturated displacements and dry entropy surfaces in unsaturated displacements. Averaging water vapor fluxes along moist entropy surfaces may give a better approximation of the Lagrangian water vapor fluxes. We have experimented with averages of water vapor fluxes along moist entropy surfaces (equivalent potential temperature surfaces). Particularly in the tropical troposphere, however, moist entropy often does not increase monotonically with height, so using moist entropy surfaces as vertical coordinate surfaces is problematic. The difference between the zonal-mean potential temperature and equivalent potential temperature in the region of the subtropical relative humidity minima is less than 8 K in summer and 4 K in winter, which means that the representation of water vapor fluxes between the subtropics and extratropics is similar in dry and moist isentropic coordinates. For the subtropical and extratropical free troposphere, the water vapor fluxes along dry

entropy surfaces presented below are qualitatively similar to the fluxes along moist entropy surfaces.

3. Data and methods

a. Data

We analyzed mean fields and fluxes of water vapor in ECMWF 40-yr Re-Analysis (ERA-40) data for the years 1980–2001, a period for which satellite data are available and are taken into account in the reanalysis (Uppala et al. 2005). Dynamical fields in the reanalysis data are represented spectrally, with triangular truncation at total wavenumber 159. Specific humidity is represented on a corresponding reduced Gaussian grid, with a spacing of about 1.1° in latitude. The fields are given on 60 vertical sigma levels (Kållberg et al. 2004).

For the computation of water vapor and other flow fields, we transformed spectral fields to the corresponding regular Gaussian grid and interpolated specific humidity to the same grid. We then interpolated to isentropic coordinates and computed averages from four-times-daily data.

The ERA-40 data currently represent the highest-resolution dataset that provides water vapor and dynamical fields with continuous long-term coverage. It appears to be the most reliable reanalysis dataset available for studies of global water vapor fields and fluxes and their vertical structure. The representation of water vapor fields in ERA-40 is improved compared with earlier reanalyses, but significant uncertainties and biases remain. See, for example, Cau et al. (2005), Ruiz-Barradas and Nigam (2005), Sudradjat et al. (2005), Trenberth and Smith (2005), Trenberth et al. (2005), and Uppala et al. (2005) for comparisons of ERA-40 data with other reanalyses and with independent data. These studies suggest that at least the qualitative results we derive based on ERA-40 data are likely to be robust. For example, it appears the ERA-40 data capture the specific humidity structure of filamentary dry intrusions from the subtropics and extratropics into the tropical troposphere (Cau et al. 2005), intrusions that may play a role in the water vapor transport between the Tropics and extratropics. A quantitative assessment of errors in our results will have to await more detailed comparisons of ERA-40 data with independent data. However, for the study of eddy fluxes of water vapor, errors in specific humidity lead to errors in the estimated eddy fluxes only inasmuch as they correlate with the advecting velocities. Relative errors in eddy fluxes—quantities of primary interest in this study—can be expected to be smaller than relative errors in specific humidities, the quantities in the reanalysis likely affected by the largest errors.

b. Saturation vapor pressure and relative humidity

For the calculation of the relative humidity, we calculated the saturation vapor pressure according to the modified Tetens formula used by ECMWF. The saturation vapor pressure is the saturation vapor pressure over ice for temperatures below −23°C, the saturation vapor pressure over liquid water for temperatures over 0°C, and a quadratic interpolation between the saturation vapor pressures over ice and liquid water for intermediate temperatures (Simmons et al. 1999). Mean relative humidities are mass-weighted isentropic averages $\overline{H}^*$ of the instantaneous ratio $H = e/e_s$ of water vapor pressure e to saturation vapor pressure e_s.

c. Interpolation to isentropic coordinates

We interpolated water vapor and other flow fields columnwise from the 60 reanalysis sigma levels to 120 isentropic levels. As isentropic levels, we used levels of constant dry potential temperature $\theta = T(p_0/p)^\kappa$, where $p_0 = 10^5$ Pa is the reference pressure and $\kappa = R/c_p$ is the adiabatic exponent, calculated with the gas constant R and specific heat c_p of dry air. That is, we neglect the small modification (less than 0.2% in the free troposphere) of the adiabatic exponent of air by water vapor. The isentropic levels are equally spaced in the transformed potential temperature coordinate $\theta^{-1/\kappa}$, with the lowermost and uppermost isentropic levels corresponding to potential temperatures of 210 and 600 K (cf. Juckes et al. 1994). (In an isothermal dry atmosphere, isentropic levels equally spaced in the transformed potential temperature coordinate $\theta^{-1/\kappa}$ would be equally spaced in pressure).

We interpolated pressure from sigma levels to isentropic levels using a locally monotonic Hermite interpolant that is piecewise cubic in $\theta^{-1/\kappa}$ (Fritsch and Butland 1984). To obtain isentropic-coordinate representations of other flow fields, such as specific humidities, specific humidity fluxes, and mass fluxes, we interpolated their mass-weighted vertical integrals over sigma levels linearly in pressure to isentropic levels, in such a way that the mass-weighted vertical integrals of the instantaneous flow fields over sigma levels are equal to the corresponding mass-weighted vertical integrals over isentropic levels (cf. Juckes et al. 1994). Using a centered difference scheme for differentiation, we obtained mass-weighted flow fields on isentropic levels from the interpolated integrals and averaged them zonally and temporally. This way of interpolating and averaging isentropic flow fields ensures that vertical integrals, for example, of specific humidities and specific humidity fluxes, are conserved to the same degree on isentropic levels as on sigma levels (except for the trun-

cation error arising because the isentropic levels do not extend to the top of the atmosphere, which is inconsequential for our analyses of tropospheric flow fields).

d. Estimation of diabatic heating rates

We estimated the mean diabatic heating rate $\overline{Q}^*$ as residual from the mean mass balance equation in isentropic coordinates,

$$\partial_t \overline{\rho}_\theta + \partial_y(\overline{\rho}_\theta \overline{v}^*) + \partial_\theta(\overline{\rho}_\theta \overline{Q}^*) = 0. \quad (4)$$

Integrating vertically from the nominal lower boundary θ_b to potential temperature θ, expressing the meridional divergence in spherical coordinates, and introducing the vertical integral of the meridional mass flux along isentropes

$$\Psi(\phi, \theta) = 2\pi a \cos\phi \int_{\theta_b}^{\theta} \overline{\rho}_\theta \overline{v}^* \, d\theta, \quad (5)$$

one obtains the mean cross-isentropic mass flux at latitude ϕ and potential temperature θ

$$\overline{\rho}_\theta \overline{Q}^* = -\frac{1}{2\pi a^2 \cos\phi} \partial_\phi \Psi(\phi, \theta) - g^{-1} \partial_t [\overline{p}_s(\phi) - \overline{p}(\phi, \theta)], \quad (6)$$

where $\overline{p}_s(\phi) = \overline{p}(\phi, \theta_b)$ is the mean surface pressure at latitude ϕ. In a statistically steady state, Ψ is the streamfunction of the mean mass flux along and across isentropes; the explicit time derivative on the right-hand side of relation (6) vanishes, and (6) reduces to the usual relation between a vertical mass flux and a meridional streamfunction. We refer to Ψ as a streamfunction, understood as defined by the integral (5) of the meridional mass flux, even when the mean state is time-dependent.

We calculated the streamfunction (5) of the isentropic mean mass flux from sigma-coordinate integrals of mass fluxes interpolated to isentropic coordinates and estimated the mean cross-isentropic mass flux as residual according to relation (6). The averages we consider are seasonal means. We estimated the explicit time derivative of the mass per unit area [the second term on the right-hand side of relation (6)] from pressure differences averaged over 20 days centered on the beginning and end of each season. In the free troposphere, the estimated explicit time derivatives typically lead to a modification of the mean cross-isentropic mass flux obtained from the streamfunction [the first term on the right-hand side of relation (6)] of up to about 15% of its minimum value in the descending branches of the Hadley circulation.

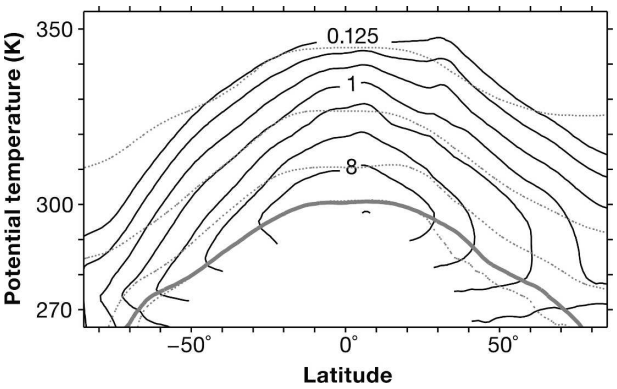

FIG. 1. Annually averaged specific humidity $\overline{q}^*$. The contouring is logarithmic, with contours at $(2^{-3}, 2^{-2}, \ldots) \times 1$ g kg^{-1}. Here and in subsequent figures, the solid gray line is the median surface potential temperature, and the dotted lines are the 250-, 500-, 750-, and 925-hPa pressure contours.

We did not have access to the instantaneous diabatic heating rate Q from the reanalysis and were unable to estimate it reliably enough as residual from other flow fields to obtain a sufficiently accurate estimate of the cross-isentropic eddy flux $\overline{Q'q'}^*$ of specific humidity. Therefore, we will not consider this term in the mean water vapor balance equation (3) individually but together with the source-sink term $\overline{S}^*$.

4. Zonal-mean climatologies

a. Water vapor fields

Figure 1 shows the zonally and annually averaged specific humidity $\overline{q}^*$. In this and in subsequent figures, the contouring is logarithmic, to be able to display water vapor fields and fluxes in the upper and lower troposphere simultaneously. A few contours of the mean pressure $\overline{p}$ on isentropes are shown as height and temperature indicators. In the calculation of the mean pressure $\overline{p}$, we used Lorenz's (1955) convention of setting the pressure on isentropes inside the surface to the instantaneous surface pressure, $p(\theta < \theta_s) = p_s$, so that the relation $\overline{\rho}_\theta = -g^{-1}\partial_\theta \overline{p}$ between mean isentropic density and mean pressure holds throughout the flow domain in isentropic coordinates. At the lower boundary of the isentropic domain, the mean pressure $\overline{p}$ then approaches the mean surface pressure $\overline{p}_s$. Specific humidity contours near the lower boundary are truncated at the 1% isoline of the latitude-dependent cumulative distribution of surface potential temperatures, that is, at the potential temperature below which the surface potential temperature at any given latitude lies 1% of the time.

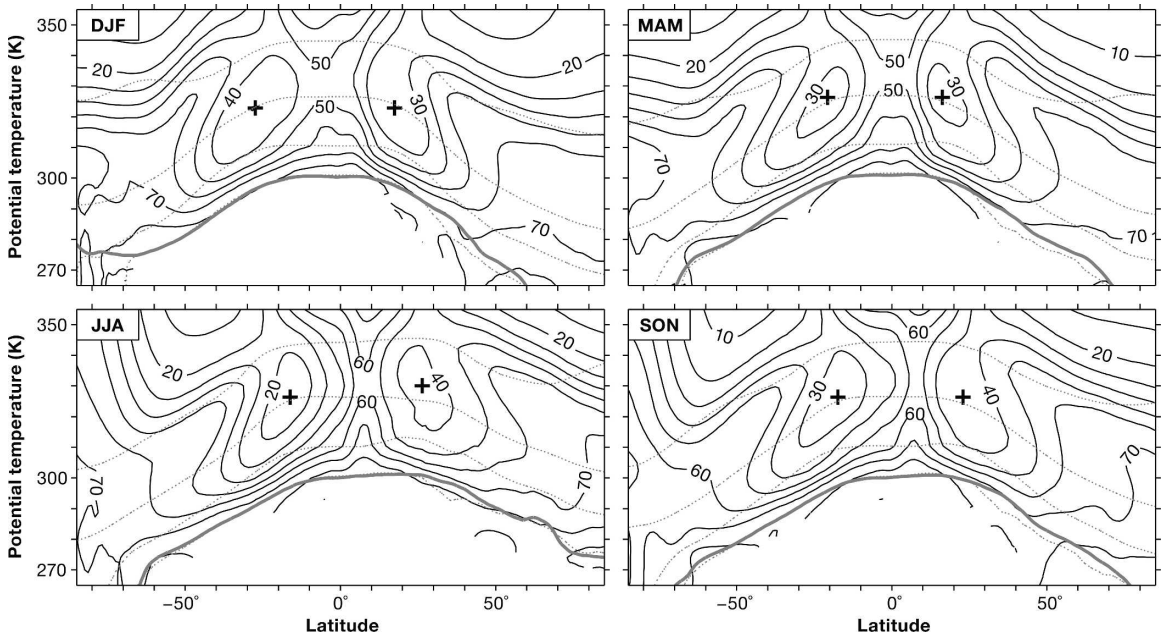

FIG. 2. Seasonally averaged relative humidity $\overline{H}^*$ (percent). The crosses mark the relative humidity minima in the subtropical free troposphere.

In the free troposphere, specific humidity generally decreases upward across and poleward along isentropes, consistent with the upward and poleward decrease of temperature. An exception is a region of about 10° width at about 30°N in the upper troposphere, in which specific humidity increases poleward along isentropes. This narrow region of reversed isentropic specific humidity gradients in the upper troposphere is primarily associated with the relatively high summer temperatures and specific humidities on isentropes in the Asian monsoon region. The general poleward decrease of specific humidity along isentropes in the free troposphere implies that water vapor is not mixed along isentropes like a conserved passive scalar but that, as is well known, water vapor is lost through condensation in poleward displacements of air masses along isentropes.

Near the lower boundary, specific humidity increases upward across isentropes because the mass-weighted mean temperature $\overline{T}^*$ increases with potential temperature there. In the surface layer of isentropes that sometimes intersect the surface at a fixed latitude, the mean temperature at a given potential temperature contains contributions from all instances and longitudes at which the surface potential temperature is less than the given potential temperature. At the minimum surface potential temperature, the mean temperature is approximately equal to the minimum surface potential temperature. At a higher potential temperature in the surface layer, the mean temperature can be higher because it contains contributions from the instances and longitudes at which the surface potential temperature is equal to the higher potential temperature. Therefore, since relative humidity variations near the surface do not compensate the temperature variations, specific humidity increases upward across isentropes near the lower boundary.

Figure 2 shows the seasonally averaged relative humidity $\overline{H}^*$ for the December–January–February (DJF), March–April–May (MAM), June–July–August (JJA), and September–October–November (SON) seasons, revealing the structure and seasonal variations of subsaturated regions. Near the lower boundary, relative humidity contours are truncated in the same way as the contours in Fig. 1. For later reference, the relative humidity minima in the subtropical free troposphere are marked by crosses. The relative humidity minima are located at potential temperatures between 320 and 330 K (corresponding to mean pressures of 430–520 hPa). The relative humidities at the subtropical minima are smaller in the winter hemisphere than in the summer hemisphere, a feature already documented by Peixoto and Oort (1996).

In the free troposphere outside the Tropics and subtropics, the relative humidity generally increases poleward along isentropes, consistent with eddies advecting moist air masses into colder regions poleward on isentropes, where water vapor condenses and precipitates

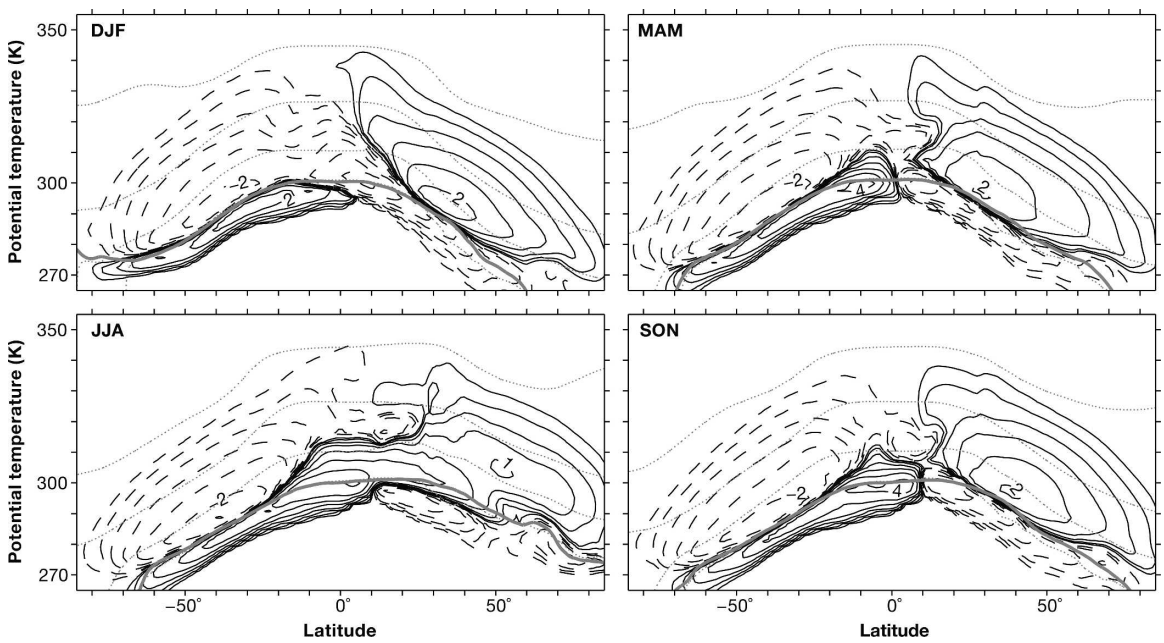

FIG. 3. Seasonally averaged total flux $\overline{\rho}_\theta\,\overline{v}\overline{q}^*$ of specific humidity along isentropes. The contouring is logarithmic, with contours at $\pm(2^{-4}, 2^{-3}, \ldots) \times 1$ kg m^{-1} K^{-1} s^{-1}. Negative contours are dashed.

(cf. Kelly et al. 1991; Yang and Pierrehumbert 1994). If temperature decreases monotonically poleward along isentropes, the relative humidity of air masses that have passed through colder poleward regions on isentropes, when they return to lower latitudes, will be lower the greater the meridional distance to their latitude of last saturation. Hence, one would expect the relative humidity in the free troposphere to increase monotonically poleward along isentropes, roughly as in Fig. 2, provided that temperature decreases monotonically along isentropes, that displacements in large-scale eddies are approximately confined to isentropes, and that eddy fluxes dominate the isentropic water vapor transport. As seen in Fig. 2, the cold polar regions are subsaturated (relative to the saturation vapor pressure over ice in sufficiently cold regions, as described in section 3b). This indicates that either or both of two dynamical processes are acting there: (i) eddy temperature fluctuations in time or along a latitude circle with attendant condensation and precipitation at the lowest temperatures lead to mean subsaturation; (ii) subsidence and admixture of dry air masses from higher altitudes lead to mean subsaturation.

To investigate the transport processes that balance the difference between the rates of evaporation and precipitation at the surface and that contribute to the maintenance of the global distribution of water vapor in the troposphere, we next consider seasonally averaged water vapor fluxes along and across isentropes.

b. Water vapor fluxes along isentropes

Figure 3 shows the meridional specific humidity flux along isentropes, $\overline{\rho}_\theta\,\overline{v}\overline{q}^*$, weighted by the isentropic density so that the flux smoothly goes to zero at the lower boundary and its integral over potential temperature represents a flux of precipitable water. The flux is generally directed poleward in the free troposphere (in the extratropics, down to about the median or mean surface potential temperature). Near the surface, the flux is directed equatorward, with a cross-equatorial component from winter to summer hemisphere in the solstice seasons.

How the structure of the meridional specific humidity flux comes about becomes clearer when the flux is decomposed into mean and eddy components. Figure 4 shows the eddy component $\overline{\rho}_\theta\,\overline{v'q'}^*$. The eddy component includes contributions from all fluctuations about the seasonal and zonal mean and thus includes contributions from stationary eddies and intraseasonal variations. Comparison of the seasonal eddy fluxes in Fig. 4 with monthly eddy fluxes (i.e., with eddies defined as fluctuations about monthly means) shows that intraseasonal variations do not affect the magnitude and structure of the seasonal eddy fluxes substantially, with the exception of the JJA eddy fluxes, especially in the upper troposphere around 30°N, which are influenced by the seasonal evolution of monsoons.

The eddy flux of specific humidity along isentropes is

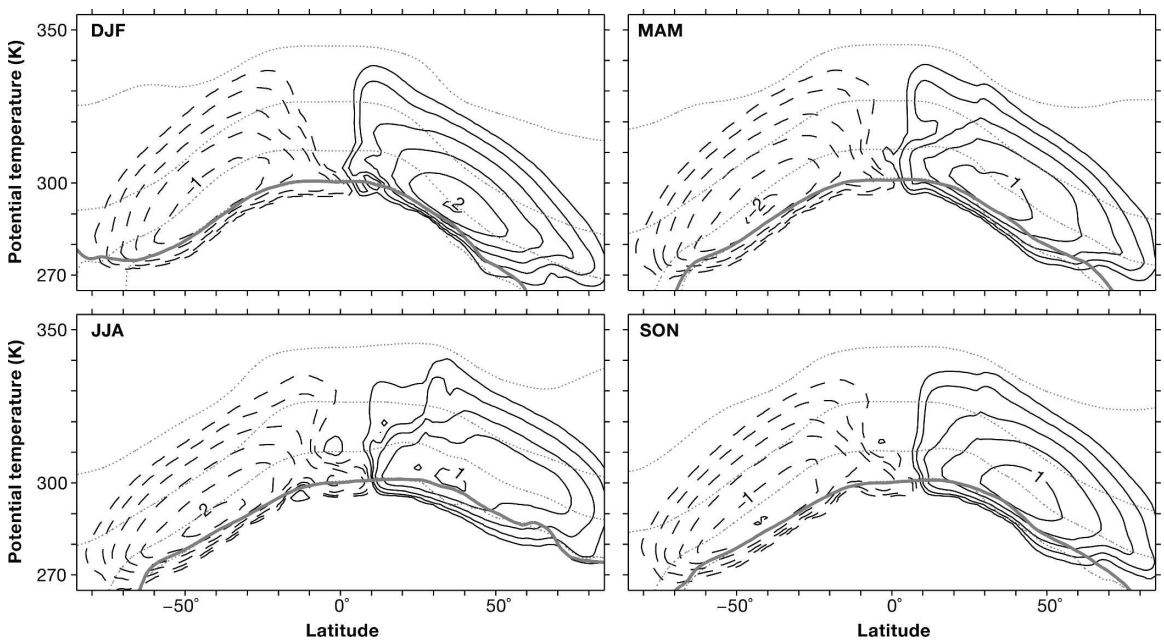

FIG. 4. Seasonally averaged eddy flux $\overline{\rho}_\theta \overline{v'q'}^*$ of specific humidity along isentropes (kg m^{-1} K^{-1} s^{-1}). The contour levels are the same as in Fig. 3.

directed from the ITCZ poleward at all levels and throughout the troposphere, with the exception of the immediate vicinity of the equator. Eddies transport water vapor from the deep Tropics through the subtropics into the extratropics (including the high latitudes). There is no obvious transition in water vapor transport regimes between low and middle latitudes, such as the weakly permeable barrier to the transport of conserved passive scalars evident in the subtropics (Pierrehumbert and Yang 1993). (Because of condensation, waves can transport water vapor across transport barriers for conserved passive scalars if condensation occurs preferentially on one side of the barrier, that is, if there is a temperature gradient across the barrier.) Especially in the Northern Hemisphere in JJA, significant eddy fluxes of specific humidity originate deep in the Tropics, near the ITCZ. The water vapor transported by the eddies from the Tropics into the subtropics and extratropics originates not only, as is sometimes assumed, near the tropopause, but at all levels.

The extratropical eddy flux of specific humidity along isentropes is stronger in the winter hemisphere than in the summer hemisphere. The increased eddy activity in the winter hemisphere overcompensates the reduction in saturation vapor pressure and specific humidity due to the lower temperatures.

Figure 5 shows the mean component $\overline{\rho}_\theta \overline{v}^* \overline{q}^*$ of the meridional flux of specific humidity along isentropes. The mean component is generally directed poleward in the free troposphere and equatorward near the surface, with a cross-equatorial component in the solstice seasons. It represents the advective flux of specific humidity associated with the mean mass flux $\overline{\rho}_\theta \overline{v}^*$ along isentropes, whose streamfunction, defined in Eq. (5), is shown in Fig. 6.

The mean mass flux along ($\overline{\rho}_\theta \overline{v}^*$) and across ($\overline{\rho}_\theta \overline{Q}^*$) isentropes forms hemispheric overturning circulations. Cross-isentropic ascent in low latitudes corresponds to diabatic heating, and cross-isentropic descent in higher latitudes to diabatic cooling. Poleward mass flux in the free troposphere and equatorward mass flux near the surface close the circulations. In the Tropics, the mean mass flux along and across isentropes is the mass flux of the Hadley circulation. In the extratropics, the mean mass flux along isentropes encompasses a contribution from the thermally indirect Ferrel cells that appear in the mean component $\overline{\rho}_\theta \overline{v}$ of the mass flux $\overline{\rho}_\theta \overline{v}^* = \overline{\rho}_\theta \overline{v}$, as in pressure or height coordinates. However, the extratropical mean mass flux along isentropes is dominated by an eddy mass flux [Tung 1986; Juckes et al. 1994; Held and Schneider 1999; Koh and Plumb 2004; Schneider 2005; see Schneider (2006) for a review]. As seen in Fig. 6 and discussed by Held and Schneider (1999), most of the equatorward mass flux in the extratropics occurs at potential temperatures below the median or mean surface potential temperature, that is, in cold-air outbreaks. The structure of the mean mass flux along isentropes imprints itself on the structure of the

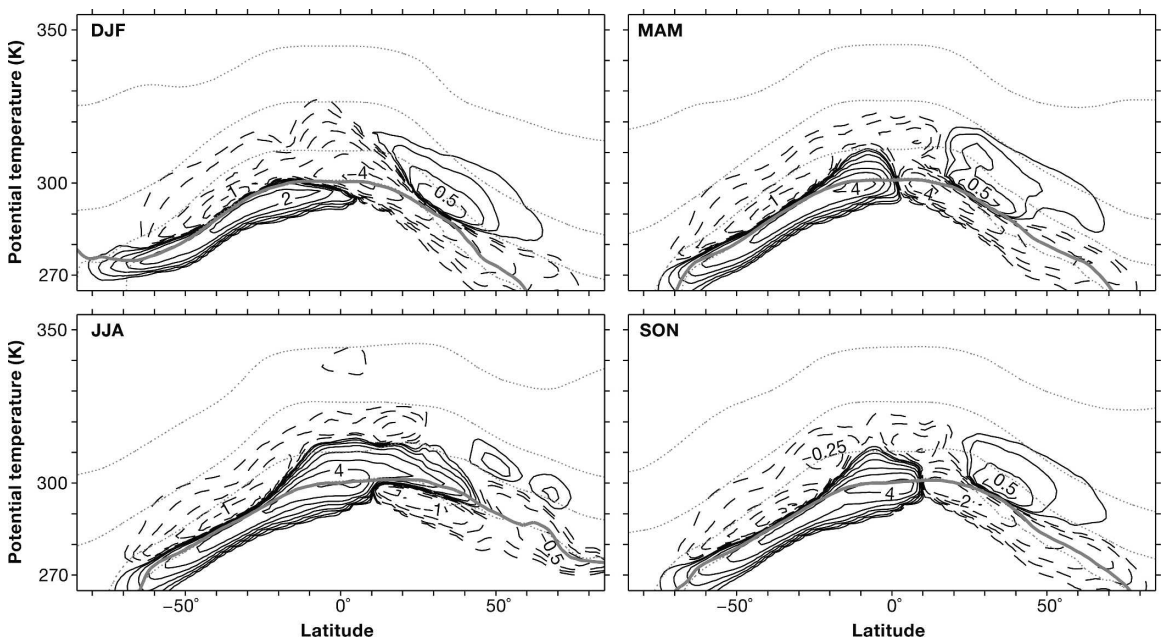

FIG. 5. Seasonally averaged mean flux $\overline{\rho}_\theta \overline{v}^* \overline{q}^*$ of specific humidity along isentropes (kg m^{-1} K^{-1} s^{-1}). The contour levels are the same as in Fig. 3.

mean advective flux of specific humidity along isentropes (cf. Figs. 5 and 6). In the extratropics, what appears in this analysis as the mean advective flux of specific humidity along isentropes is itself an aggregate of eddy motions, since the advecting mean mass flux along isentropes is primarily an aggregate of eddy motions (the mass flux of the Ferrel cell has the opposite direction).

The equatorward specific humidity flux near the surface and the cross-equatorial specific humidity flux

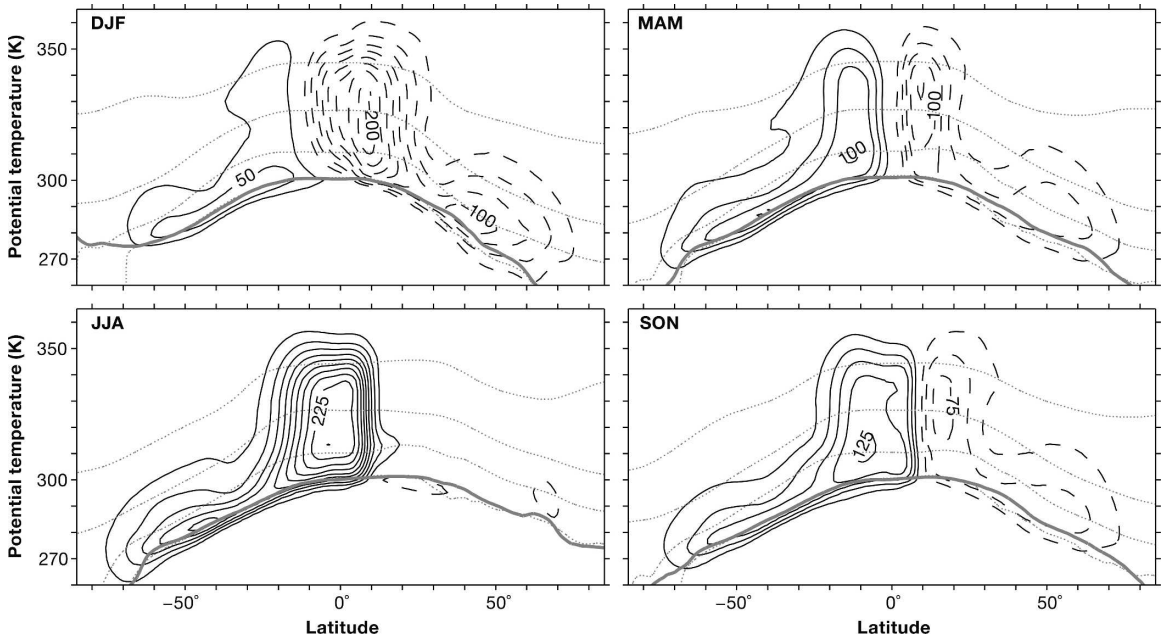

FIG. 6. Seasonally averaged streamfunction of mass flux along and across isentropes (contour interval 25 × 10^9 kg s^{-1}). Solid lines correspond to counterclockwise rotation, dashed lines to clockwise rotation.

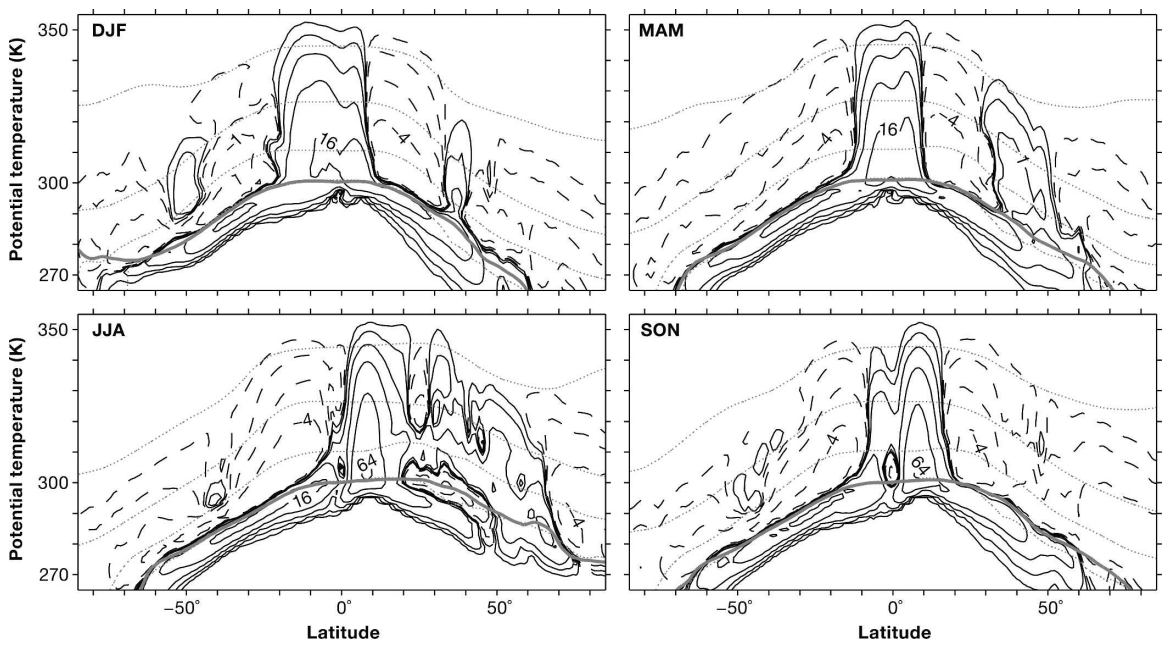

FIG. 7. Seasonally averaged mean flux $\overline{\rho}_\theta \overline{Q}^* \overline{q}^*$ of specific humidity across isentropes. The contouring is logarithmic, with contours at $\pm(4^{-2}, 4^{-1}, \ldots) \times 10^{-6}$ kg m^{-2} s^{-1}.

from winter to summer hemisphere in the solstice seasons seen in Fig. 3 can be entirely attributed to the mean advective flux of specific humidity shown in Fig. 5. The equatorward specific humidity flux along isentropes is the mean advective flux associated with the equatorward near-surface branch of the overturning mass transport circulation (Fig. 6). It transports water vapor into low latitudes and into the ITCZ. The cross-equatorial specific humidity flux along isentropes is the mean advective flux associated with the cross-equatorial near-surface branch of the Hadley circulation, which appears to be largely a manifestation of monsoons (Dima and Wallace 2003).

Comparison of Figs. 3–5 shows that, in the extratropical free troposphere, the eddy component dominates the meridional specific humidity flux along isentropes. The eddy component also dominates in the tropical upper troposphere above about 500 hPa. The mean component only dominates near the surface (in the extratropics, below the median or mean surface potential temperature). Since the mean component, where it is dominant, is directed equatorward or is cross-equatorial, this implies that, apart from the cross-equatorial transport, the bulk of the poleward transport of water vapor is affected by isentropic eddy fluxes.

c. Water vapor fluxes across isentropes

The mean mass flux $\overline{\rho}_\theta \overline{Q}^*$ across isentropes advects specific humidity vertically. Figure 7 shows the corresponding mean advective cross-isentropic flux of specific humidity, $\overline{\rho}_\theta \overline{Q}^* \overline{q}^*$.

The mean advective cross-isentropic specific humidity flux is directed upward in the ascending branch of the Hadley circulation and near the surface, where the mean meridional mass flux along isentropes is directed equatorward and thus is associated with diabatic heating (cf. Fig. 6). The cross-isentropic specific humidity flux is also directed upward in midlatitudes, particularly in the summer hemisphere and most markedly in the Northern Hemisphere. The upward cross-isentropic mass flux in midlatitudes most likely is a manifestation of latent heat release, possibly in baroclinic eddies. The latent heat release may occur in large-scale condensation or in moist convection, for example, in the warm sectors of surface cyclones in the storm tracks (cf. Hu and Liu 1998). Given that the upward mass and specific humidity fluxes are stronger in the Northern Hemisphere in JJA than in the Southern Hemisphere in DJF (the maxima of the mean cross-isentropic mass and specific humidity fluxes in midlatitudes are about a factor of 4 greater in Northern Hemisphere summer than in Southern Hemisphere summer), it is likely that the diabatic heating in Northern Hemisphere summer primarily occurs in moist convection over continents. In JJA, the cross-isentropic specific humidity flux is also directed upward at around 30°N in the middle and upper troposphere, associated with latent heat release primarily in the Asian monsoon.

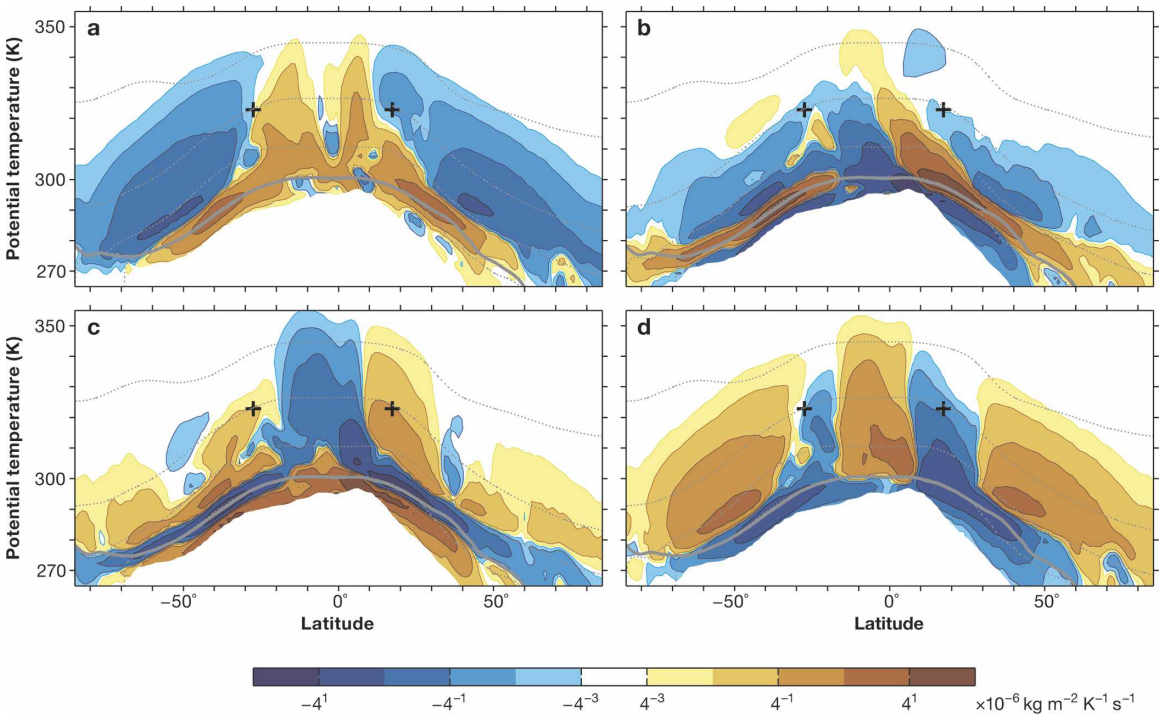

FIG. 8. Divergence of seasonally averaged water vapor flux components for DJF: (a) isentropic eddy component $\partial_y(\overline{\rho}_\theta\,\overline{v'q'}^*)$; (b) isentropic mean component $\partial_y(\overline{\rho}_\theta\,\overline{v}^*\,\overline{q}^*)$; (c) cross-isentropic mean component $\partial_\theta(\overline{\rho}_\theta\,\overline{Q}^*\,\overline{q}^*)$; (d) residual $\partial_\theta(\overline{\rho}_\theta\,\overline{Q'q'}^*) - \overline{\rho}_\theta\,\overline{S}^*$. The crosses mark the relative humidity minima in the subtropical free troposphere (cf. Fig. 2). Near the lower boundary, divergence contours are truncated at the 1% isoline of the latitude-dependent cumulative distribution of surface potential temperatures.

In other regions of the extratropics, the mean advective cross-isentropic specific humidity flux is directed downward, associated with radiative cooling and corresponding downward cross-isentropic mass fluxes. We did not evaluate the cross-isentropic eddy flux of specific humidity, $\overline{\rho}_\theta\,\overline{Q'q'}^*$, which contributes to the vertical redistribution of water vapor.

d. Divergence of water vapor fluxes

Integrated over potential temperature, the terms involving derivatives with respect to potential temperature vanish, and the mean balance equation (3) for water vapor becomes a mean balance equation for precipitable water. In a statistically steady state, the divergence of the horizontal fluxes balances the difference between the zonal-mean rates of evaporation $\overline{E}$ and precipitation $\overline{P}$ at the surface, $\overline{E} - \overline{P} = \int_{\theta_b}^{\infty} \overline{\rho}_\theta \overline{S}^*\,d\theta$ (provided subgrid-scale horizontal dispersion of water vapor and horizontal transport and evaporation of condensate do not contribute significantly to the mean source-sink term). The structure of the horizontal divergence terms in the balance equation (3) thus gives information on the relative contributions of isentropic mean and eddy transports to balancing the distribution of $\overline{E} - \overline{P}$. Similarly, the structure of the vertical divergence terms gives information on the cross-isentropic redistribution of water vapor. Divergence or convergence of a flux term in an atmospheric region can be interpreted as a tendency of the associated transport process to dry or moisten the region.

Figures 8–11 show terms in the seasonally averaged balance equation (3) for DJF, MAM, JJA, and SON. In each figure, panel (a) shows the meridional divergence of the isentropic eddy flux component $\partial_y(\overline{\rho}_\theta\,\overline{v'q'}^*)$, panel (b) the meridional divergence of the isentropic mean flux component $\partial_y(\overline{\rho}_\theta\,\overline{v}^*\,\overline{q}^*)$, panel (c) the vertical divergence of the cross-isentropic mean component $\partial_\theta(\overline{\rho}_\theta\,\overline{Q}^*\,\overline{q}^*)$, and panel (d) the residual

$$-[\partial_t(\overline{\rho}_\theta\,\overline{q}^*) + \partial_y(\overline{\rho}_\theta\,\overline{vq}^*) + \partial_\theta(\overline{\rho}_\theta\,\overline{Q}^*\overline{q}^*)]$$
$$= \partial_\theta(\overline{\rho}_\theta\,\overline{Q'q'}^*) - \overline{\rho}_\theta\,\overline{S}^*.$$

The explicit time derivative $\partial_t(\overline{\rho}_\theta\,\overline{q}^*)$ was estimated from differences in the density-weighted specific humidities $\overline{\rho}_\theta\,\overline{q}^*$ averaged over 20 days centered on the beginning and end of each season. All other derivatives were estimated using second-order centered differences.

Isentropic eddy fluxes of specific humidity, $\overline{v'q'}^*$, generally diverge near the surface and in the tropical

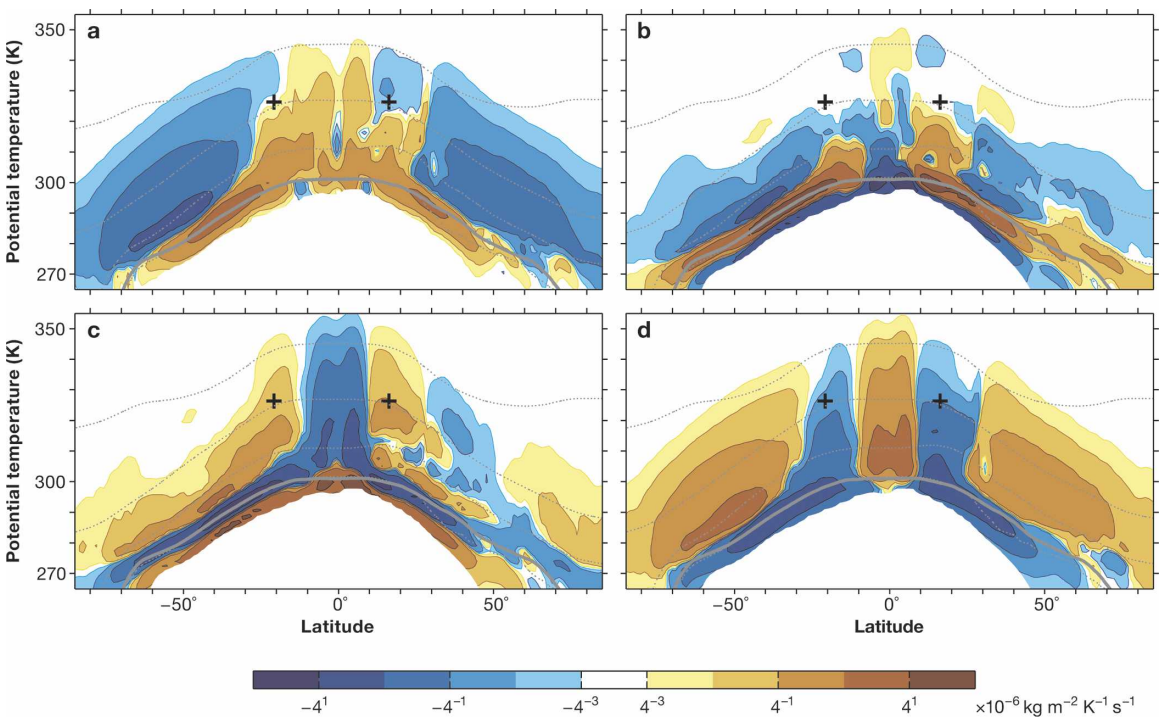

FIG. 9. Same as Fig. 8, but for MAM.

and subtropical free troposphere; they converge in the extratropical free troposphere [panel (a) of Figs. 8–11]. Thus, isentropic eddy fluxes transport water vapor from all levels in the Tropics and from near-surface levels throughout the atmosphere into the extratropical free troposphere. They represent the largest contribution to the convergence of water vapor fluxes in the extratropical free troposphere. Strong divergence of isentropic

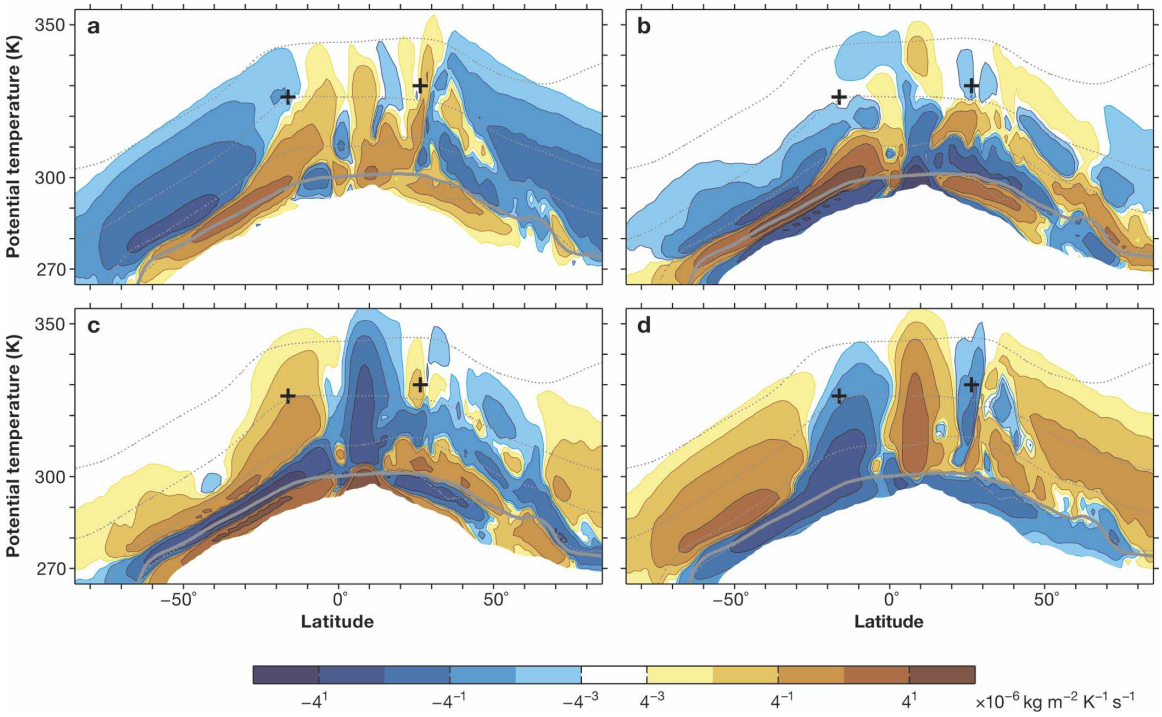

FIG. 10. Same as Fig. 8, but for JJA.

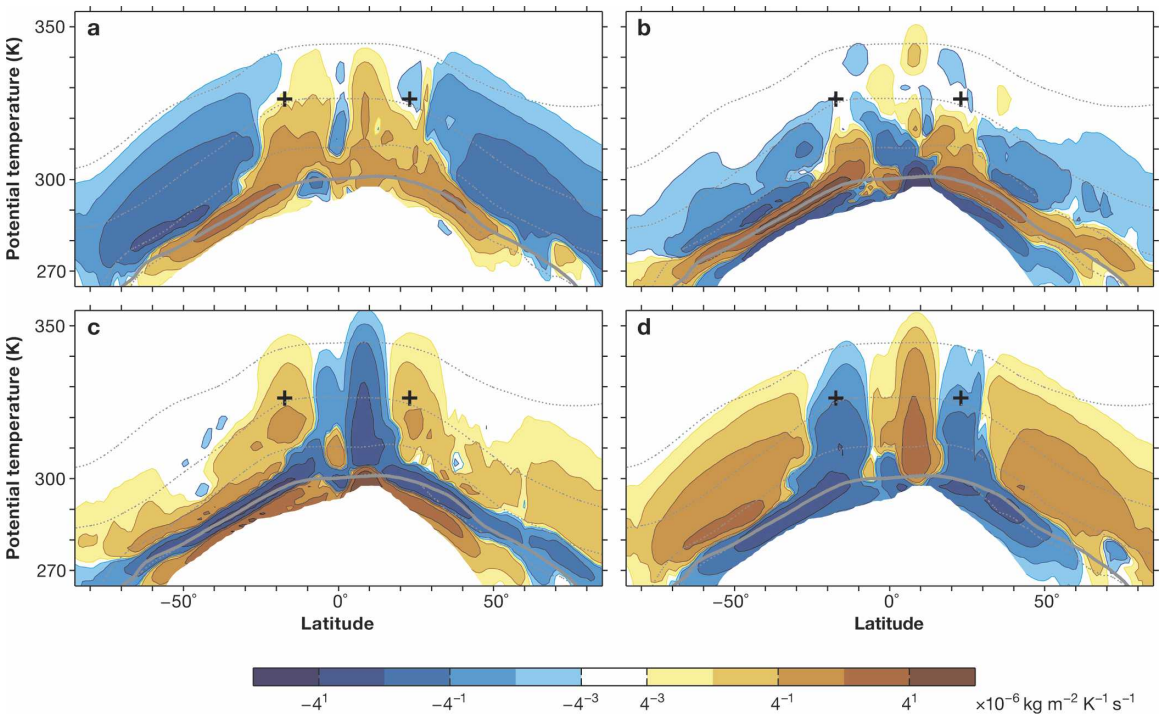

FIG. 11. Same as Fig. 8, but for SON.

eddy fluxes of specific humidity extends deep into the Tropics, up to the ITCZ. Near the subtropical relative humidity minima (marked by crosses), the divergence of isentropic eddy fluxes of specific humidity is not of a consistent sign in all seasons and is generally small in magnitude compared with the divergence of the cross-isentropic mean advective flux [cf. panels (a) and (c) of Figs. 8–11]. Although there are significant isentropic eddy fluxes of specific humidity through the region of the subtropical relative humidity minima (cf. Fig. 4), moistening by eddy transport from the Tropics into the region of the minima approximately balances drying by eddy transport into the extratropics. There is no strong net drying or moistening tendency near the subtropical relative humidity minima owing to isentropic eddy fluxes.

Convergence of isentropic mean advective fluxes of specific humidity, $\overline{v}^*\overline{q}^*$, contributes to the moistening of the extratropical free troposphere, but the magnitude of this convergence is generally smaller than that of the convergence of isentropic eddy fluxes [cf. panels (a) and (b) of Figs. 8–11]. However, the magnitude of the divergence of isentropic mean advective fluxes near the surface, where they transport water vapor toward and across the equator (cf. Fig. 5), can be larger than that of the isentropic eddy fluxes.

Cross-isentropic mean advective fluxes of specific humidity, $\overline{Q}^*\overline{q}^*$, generally converge in the Tropics, in the ascending branches of the Hadley circulation, and diverge in the extratropical free troposphere, in regions of mean cross-isentropic subsidence [panel (c) of Figs. 8–11]. Near the surface, they diverge at the lowest levels and converge near the top of the planetary boundary layer, consistent with diabatic heating near the surface and, predominantly, diabatic cooling aloft (cf. Fig. 7). Cross-isentropic mean advective fluxes of specific humidity represent a significant water vapor source for the extratropical and parts of the subtropical free troposphere in summer, especially in the Northern Hemisphere (Fig. 10c). Near the subtropical relative humidity minima, the divergence of cross-isentropic mean advective fluxes of specific humidity represents the largest drying tendency in the balance equation (3), particularly in the descending branches of the strong winter Hadley cells [panel (c) of Figs. 8 and 10].

Where the residual $\partial_\theta(\overline{\rho}_\theta\,\overline{Q'q'}^*) - \overline{\rho}_\theta\,\overline{S}^*$ is positive, the mean local condensation rate exceeds the mean local evaporation rate plus any convergence of cross-isentropic turbulent (eddy and subgrid-scale) fluxes of water vapor; where it is negative, the mean local evaporation rate exceeds the mean local condensation rate plus any divergence of cross-isentropic turbulent fluxes. In the free troposphere, cross-isentropic turbulent fluxes of water vapor, if they are significant at all, can be expected to converge, corresponding to water vapor transport down the mean vertical gradient from near

the surface into the free troposphere. So if the contribution of subgrid-scale horizontal dispersion to the mean specific humidity balance is small (which we assume in what follows), positive values of the residual in the free troposphere usually indicate mean condensation. Negative values of the residual in the free troposphere usually indicate mean convergence of cross-isentropic turbulent fluxes, potentially plus mean evaporation of condensate.

The residual is generally negative near the surface, indicating mean evaporation [panel (d) of Figs. 8–11]. The residual is also negative in the subtropical free troposphere, indicating convergence of cross-isentropic turbulent fluxes, potentially plus evaporation of condensate. To the extent that evaporation of condensate represents a small contribution to the residual, the convergence of cross-isentropic turbulent fluxes is what primarily balances the divergence of the cross-isentropic mean advective fluxes of specific humidity near the subtropical relative humidity minima [cf. panels (c) and (d) of Figs. 8–11]. Turbulent boundary layer fluxes and shallow convection will contribute to the cross-isentropic turbulent fluxes in the lower troposphere, but near the relative humidity minima, well above the planetary boundary layer (at pressures of about 500 hPa), the cross-isentropic turbulent fluxes are likely associated with convective clouds penetrating into the middle and upper troposphere. In the tropical and extratropical free troposphere, the residual is generally positive, indicating mean condensation. Integrated over potential temperature, the residual indicates the familiar pattern of excess of precipitation over evaporation in the Tropics and extratropics and excess of evaporation over precipitation in the subtropics (cf. Peixoto and Oort 1992, chapter 12.3.3).

5. Conclusions and implications

We have presented a climatology of zonal-mean water vapor fields and fluxes in isentropic coordinates. The analyses revealed the significance of large-scale eddy fluxes of water vapor along isentropes, not only in the extratropics, but also in the deep Tropics. At all levels, isentropic eddy fluxes transport water vapor from the deep Tropics through the subtropics into the extratropics. Isentropic eddy fluxes of specific humidity diverge near the surface and in the subtropical and tropical troposphere, including near the ITCZ; they converge in the extratropical free troposphere. Near the relative humidity minima in the subtropical free troposphere, the divergence of isentropic eddy fluxes of specific humidity is relatively small. This implies that moistening by eddy transport from the Tropics into the region of the relative humidity minima approximately balances drying by eddy transport into the extratropics, so that, near the minima, there is no strong net drying or moistening tendency owing to isentropic eddy fluxes. The dominant divergence in the mean specific humidity balance near the relative humidity minima is the divergence of the cross-isentropic mean advective flux of specific humidity in the descending branches of the Hadley circulation. This divergence is primarily balanced by convergence of cross-isentropic turbulent fluxes, which transport water vapor from the surface into the middle and upper troposphere. Cross-isentropic mean advective fluxes of specific humidity are also important in the ascending branches of the Hadley circulation, where they are associated with moist convection and moisten the free troposphere, and in the extratropics in summer, especially in the Northern Hemisphere, where they appear to be associated primarily with moist convection over continents and represent a significant moisture source for the free troposphere. Isentropic mean advective fluxes of specific humidity dominate the meridional flux of specific humidity near the surface, where they transport water vapor equatorward and, in the solstice seasons, across the equator.

Earlier accounts of how the subtropical relative humidity minima are maintained need to be amended. It has been suggested that isentropic eddy fluxes of water vapor from the subtropics into the extratropics dry the subtropics (Kelly et al. 1991; Yang and Pierrehumbert 1994; Galewsky et al. 2005) and that isentropic eddy fluxes from the Tropics into the subtropics moisten the subtropics (Emanuel and Pierrehumbert 1995; Pierrehumbert 1998; Pierrehumbert and Roca 1998). Our analysis suggests that, in the zonal mean albeit not necessarily locally, these processes balance approximately.[1] The dominant terms in the specific humidity balance near the subtropical relative humidity minima

[1] Although Galewsky et al. (2005), based on their Lagrangian transport study, emphasize the role of isentropic eddy fluxes in drying the subtropical free troposphere, their results appear to be qualitatively consistent with ours. Galewsky et al. found that, in DJF 2001–02 in the Northern Hemisphere, about half of the air in the region of the subtropical relative humidity minima was last saturated poleward of the minima, primarily at points lying on the mean isentropes going through the minima. This implies an isentropic water vapor flux from the subtropics into higher latitudes. The isentropic eddy flux of water vapor from the Tropics into the subtropics and the upward cross-isentropic turbulent fluxes in the subtropics revealed in our analysis appear in the study of Galewsky et al. as a flux of a "source tracer" that tracks the transport of water vapor from evaporation sources at the surface and contributes significantly to the specific humidity of the subtropics (J. Galewsky and A. Sobel 2005, personal communication).

are the drying tendency owing to mean subsidence and the moistening tendency owing to cross-isentropic turbulent transport of water vapor from the surface upward. The precise nature of the cross-isentropic turbulent fluxes transporting water vapor from the surface into the middle and upper troposphere in the subtropics is unclear. Water vapor fluxes in the boundary layer and in shallow convection are certain to play a role, but given that the subtropical relative humidity minima are located well above the planetary boundary layer, water vapor fluxes in convective clouds above the planetary boundary layer also appear to be significant. These results accord a central role to cloud dynamics in controlling the relative humidity of the subtropical free troposphere.

Since the conclusions about the water vapor balance in the subtropical free troposphere are based on reanalysis data, there are uncertainties about their validity. However, the qualitative conclusions derive from large-scale balances (particularly the relative smallness of the divergence of isentropic eddy fluxes), which, to be qualitatively in error, would require large biases in the correlation between specific humidities and meridional velocities. Biases of sufficient magnitude to call the qualitative aspects of the conclusions in question seem unlikely, but quantitative uncertainties clearly remain.

Although our analysis deemphasizes isentropic eddy fluxes as a factor responsible for net drying or moistening tendencies in the subtropics in climatological means, isentropic eddy fluxes may still be of primary importance in transient adjustments of the subtropical humidity after perturbations. For example, within days, a moist perturbation in the subtropics may be advected by large-scale eddies along isentropes into colder extratropical regions, leading to saturation and precipitation, so that the associated air mass upon its return to the subtropics will be drier. This adjustment to a drier state may be accomplished primarily by isentropic eddy fluxes even if their divergence in the climatological mean in the subtropics is small—provided the time scale of eddy transport from the subtropics into higher latitudes is smaller than the time scale of mean subsidence. More generally, in understanding how the relative humidity of the subtropical free troposphere changes as the climate changes one cannot ignore isentropic eddy fluxes of water vapor but must consider how the balance of isentropic eddy fluxes, cross-isentropic mean advective fluxes, and cross-isentropic turbulent fluxes may shift as the climate changes.

In our account of the hydrologic cycle of the troposphere, it is unclear with what dynamical processes the various isentropic and cross-isentropic large-scale eddy and turbulent fluxes are associated. Isentropic eddy fluxes of specific humidity extend from the deep Tropics into the extratropics without, from the perspective of this analysis, an obvious transition in transport regimes. While it is clear that the extratropical eddy fluxes are primarily associated with baroclinic eddies, the tropical eddy fluxes are likely associated with a combination of tropical processes, such as easterly waves, and subtropical or extratropical processes, such as dry intrusions from higher latitudes into the Tropics (Mapes and Zuidema 1996; Yoneyama and Parsons 1999; Cau et al. 2005) or "rivers" of moist air transporting water vapor from the Tropics into higher latitudes (Newell et al. 1992; Zhu and Newell 1998). Both the dry intrusions and the moist "rivers" may represent filamentary remnants or extensions into the Tropics of extratropical eddies (cf. Waugh 2005). Analyzing the three-dimensional and time-dependent structure of water vapor fields and fluxes in isentropic coordinates may help to elucidate the dynamical processes responsible for the climatological-mean fields and fluxes. It would also unmask the zonal asymmetries (e.g., monsoon regions and deserts) contributing to the zonal-mean fields on which we have focused.

Acknowledgments. We are grateful for financial support by the Davidow Discovery Fund, by a Davidow Graduate Fellowship (K. Smith), by an Alfred P. Sloan Research Fellowship, and by the National Science Foundation (Grant ATM-0450059), and for computing resources and reanalysis data provided by the National Center for Atmospheric Research (which is sponsored by the National Science Foundation). T. Schneider gratefully acknowledges discussions with Isaac Held in 2001, in which the idea to analyze water vapor fluxes in isentropic coordinates originated, and with Adam Sobel, which helped to clarify the relation between our results and those of Galewsky et al. (2005). We thank Kerry Emanuel for helpful comments on the manuscript.

REFERENCES

Cau, P., J. Methven, and B. Hoskins, 2005: Representation of dry tropical layers and their origins in ERA-40 data. *J. Geophys. Res.,* **110D,** D06110, doi:10.1029/2004JD004928.

Dessler, A. E., and S. C. Sherwood, 2000: Simulations of tropical upper tropospheric humidity. *J. Geophys. Res.,* **105D,** 20 155–20 163.

Dima, I. M., and J. M. Wallace, 2003: On the seasonality of the Hadley cell. *J. Atmos. Sci.,* **60,** 1522–1527.

Emanuel, K. A., and R. T. Pierrehumbert, 1995: Microphysical and dynamical control of tropospheric water vapor. *Clouds, Chemistry, and Climate,* NATO ASI Series I, P. J. Crutzen and V. Ramanathan, Eds., Vol. 35, Springer, 17–28.

Fritsch, F. N., and J. Butland, 1984: A method for constructing

local monotone piecewise cubic interpolants. *SIAM J. Sci. Stat. Comput.,* **5,** 300–304.

Galewsky, J., A. Sobel, and I. Held, 2005: Diagnosis of subtropical humidity dynamics using tracers of last saturation. *J. Atmos. Sci.,* **62,** 3353–3367.

Held, I. M., and T. Schneider, 1999: The surface branch of the zonally averaged mass transport circulation in the troposphere. *J. Atmos. Sci.,* **56,** 1688–1697.

Hu, H., and T. Liu, 1998: The impact of upper tropospheric humidity from Microwave Limb Sounder on the midlatitude greenhouse effect. *Geophys. Res. Lett.,* **25,** 3151–3154.

Johnson, D. R., 1989: The forcing and maintenance of global monsoonal circulations: An isentropic analysis. *Advances in Geophysics,* Vol. 31, Academic Press, 43–304.

Juckes, M. N., I. N. James, and M. Blackburn, 1994: The influence of Antarctica on the momentum budget of the southern extratropics. *Quart. J. Roy. Meteor. Soc.,* **120,** 1017–1044.

Kållberg, P., A. Simmons, S. Uppala, and M. Fuentes, 2004: The ERA-40 archive. Tech. Rep., European Centre for Medium-Range Weather Forecasts, 31 pp. [Available at www.ecmwf.int/publications.]

Kelly, K. K., A. F. Tuck, and T. Davies, 1991: Wintertime asymmetry of upper tropospheric water between the northern and southern hemispheres. *Nature,* **353,** 244–247.

Koh, T.-Y., and R. A. Plumb, 2004: Isentropic zonal average formulation and the near-surface circulation. *Quart. J. Roy. Meteor. Soc.,* **130,** 1631–1654.

Lorenz, E. N., 1955: Available potential energy and the maintenance of the general circulation. *Tellus,* **7,** 157–167.

Mapes, B., and P. Zuidema, 1996: Radiative-dynamical consequences of dry tongues in the tropical troposphere. *J. Atmos. Sci.,* **53,** 620–638.

Newell, R. E., N. E. Newell, Y. Zhu, and C. Scott, 1992: Tropospheric rivers?—A pilot study. *Geophys. Res. Lett.,* **19,** 2401–2404.

Peixoto, J. P., and A. H. Oort, 1992: *Physics of Climate.* American Institute of Physics, 520 pp.

——, and ——, 1996: The climatology of relative humidity in the atmosphere. *J. Climate,* **9,** 3443–3463.

Pierrehumbert, R. T., 1998: Lateral mixing as a source of subtropical water vapor. *Geophys. Res. Lett.,* **25,** 151–154.

——, 2002: The hydrologic cycle in deep-time climate problems. *Nature,* **419,** 191–198.

——, and R. Roca, 1998: Evidence for control of Atlantic subtropical humidity by large scale advection. *Geophys. Res. Lett.,* **25,** 4537–4540.

——, and H. Yang, 1993: Global chaotic mixing on isentropic surfaces. *J. Atmos. Sci.,* **50,** 2462–2480.

——, H. Brogniez, and R. Roca, 2006: On the relative humidity of Earth's atmosphere. *The Global Circulation of the Atmosphere: Phenomena, Theory, Challenges,* T. Schneider and A. H. Sobel, Eds., Princeton University Press, in press. [Available online at geosci.uchicago.edu/~rtp1.]

Ruiz-Barradas, A., and S. Nigam, 2005: Warm season rainfall variability over the U. S. Great Plains in observations, NCEP and ERA-40 reanalyses, and NCAR and NASA atmospheric model simulations. *J. Climate,* **18,** 1808–1830.

Salathé, E. P., Jr., and D. L. Hartman, 1997: A trajectory analysis of tropical upper-tropospheric moisture and convection. *J. Climate,* **10,** 2533–2547.

Schneider, T., 2005: Zonal momentum balance, potential vorticity dynamics, and mass fluxes on near-surface isentropes. *J. Atmos. Sci.,* **62,** 1884–1900.

——, 2006: The general circulation of the atmosphere. *Annu. Rev. Earth Planet. Sci.,* **34,** 655–688.

——, I. M. Held, and S. T. Garner, 2003: Boundary effects in potential vorticity dynamics. *J. Atmos. Sci.,* **60,** 1024–1040.

Sherwood, S. C., 1996a: Maintenance of the free-tropospheric tropical water vapor distribution. Part I: Clear regime budget. *J. Climate,* **9,** 2903–2918.

——, 1996b: Maintenance of the free-tropospheric tropical water vapor distribution. Part II: Simulation by large-scale advection. *J. Climate,* **9,** 2919–2934.

Simmons, A. J., A. Untch, C. Jakob, P. Kållberg, and P. Undén, 1999: Stratospheric water vapour and tropical tropopause temperatures in ECMWF analyses and multi-year simulations. *Quart. J. Roy. Meteor. Soc.,* **125,** 353–386.

Soden, B. J., 1998: Tracking upper tropospheric water vapor radiances: A satellite perspective. *J. Geophys. Res.,* **103D,** 17 069–17 081.

Sudradjat, A., R. R. Ferraro, and M. Fiorino, 2005: A comparison of total precipitable water between reanalyses and NVAP. *J. Climate,* **18,** 1790–1807.

Sun, D.-Z., and R. S. Lindzen, 1993: Distribution of tropical tropospheric water vapor. *J. Atmos. Sci.,* **50,** 1643–1660.

Trenberth, K. E., and L. Smith, 2005: The mass of the atmosphere: A constraint on global analyses. *J. Climate,* **18,** 864–875.

——, J. Fasullo, and L. Smith, 2005: Trends and variability in column-integrated atmospheric water vapor. *Climate Dyn.,* **24,** 741–758.

Tung, K. K., 1986: Nongeostrophic theory of zonally averaged circulation. Part I: Formulation. *J. Atmos. Sci.,* **43,** 2600–2618.

Uppala, S. M., and Coauthors, 2005: The ERA-40 re-analysis. *Quart. J. Roy. Meteor. Soc.,* **131,** 2961–3012.

Waugh, D. W., 2005: Impact of potential vorticity intrusions on subtropical upper tropospheric humidity. *J. Geophys. Res.,* **110D,** D11305, doi:10.1029/2004JD005664.

Yang, H., and R. T. Pierrehumbert, 1994: Production of dry air by isentropic mixing. *J. Atmos. Sci.,* **51,** 3437–3454.

Yoneyama, K., and D. Parsons, 1999: A proposed mechanism for the intrusion of dry air into the tropical western Pacific region. *J. Atmos. Sci.,* **56,** 1524–1546.

Zhu, Y., and R. E. Newell, 1998: A proposed algorithm for moisture fluxes from atmospheric rivers. *Mon. Wea. Rev.,* **126,** 725–735.